An inverse random source scattering problem in inhomogeneous media

2011 Inverse Problems 27 035004

(http://iopscience.iop.org/0266-5611/27/3/035004)

Inverse Problems **27** (2011) 035004 (22pp) doi:10.1088/0266-5611/27/3/035004

An inverse random source scattering problem in inhomogeneous media

Peijun Li

Department of Mathematics, Purdue University, West Lafayette, IN 47907, USA

E-mail: lipeijun@math.purdue.edu

Received 27 August 2010, in final form 16 December 2010
Published 4 February 2011
Online at stacks.iop.org/IP/27/035004

Abstract

Consider the scattering problem for the one-dimensional stochastic Helmholtz equation in a slab of an inhomogeneous medium, where the source function is driven by the Wiener process. To determine the random wave field, the direct problem is equivalently formulated as a two-point stochastic boundary value problem. This problem is shown to have pathwise existence and uniqueness of a solution. Furthermore, the solution is explicitly deduced with an integral representation by solving the two-point boundary value problem. Since the source and hence the radiated field are stochastic, the inverse problem is to reconstruct the statistical structure, such as the mean and the variance, of the source function from physically realizable measurements of the radiated field on the boundary point. Based on the constructed solution for the direct problem, integral equations are derived for the reconstruction formulas, which connect the mean and the variance of the random source to those of the measured field. Numerical examples are presented to demonstrate the validity and effectiveness of the proposed method.

(Some figures in this article are in colour only in the electronic version)

1. Introduction

The inverse source scattering problem for wave propagation is largely motivated by medical applications in which it is desirable to use the measurements of electric or magnetic field on the surface of the human body, such as the head, to infer the source currents inside the body, such as the brain, that produced these measured data. It has been considered as a basic tool for the solution of reflection tomography, diffusion-based optical tomography, and more recently fluorescence microscopy [29], where the fluorescence in the specimen, such as green fluorescent protein, gives rise to emitted light which is focused to the detector by the same objective that is used for the excitation. In addition, the inverse source problem has attracted much research in the antenna community [12]. A variety of antenna-embedding materials

or substrates, including plasmas, non-magnetic dielectrics, magneto-dielectrics, and, more recently, double negative meta-materials are of interest.

The problem has been extensively investigated and there is much work on the scalar and the full vector electromagnetic inverse source problems in the free space as well as in nonhomogeneous background media, see e.g. Albanese and Monk [1], Ammari *et al* [2], Eller and Valdivia [14], Marengo *et al* [23], and references cited therein. It is also known that the inverse source problem does not have a unique solution due to the possible existence of nonradiating sources, see e.g. Bleistein and Cohen [8], Devaney and Sherman [13], and Hauer *et al* [17]. In order to obtain a unique solution, it is necessary to give additional constraints that the source must satisfy. A typical choice of the constraint is to take the minimum energy solution, which represents the pseudo-inverse solution for the inverse source problem, see e.g. Marengo and Devaney [22]. See also Bao *et al* [7] for a multi-frequency inverse source problem in which the uniqueness is shown and some stability estimates are established from the radiated fields outside the source volume for a set of frequencies. A complete account of the general theory of inverse scattering problems may be found in Colton and Kress [10].

In this paper, we study the inverse random source scattering problem for the one-dimensional Helmholtz equation in a slab of the inhomogeneous medium, which is to reconstruct the statistical characteristics of the random source function. Since the source, and hence the radiated field, are modeled by random processes, the governing Helmholtz equation is considered as a stochastic differential equation instead of its deterministic counterpart.

Stochastic inverse problems refer to inverse problems that involve uncertainties and randomness. Compared to classical inverse problems, stochastic inverse problems have substantially more difficulties on top of the existing hurdles, mainly due to the involved randomness and uncertainties. For instance, unlike the deterministic nature of solutions for classical inverse problems, the solutions for a stochastic inverse problem are random functions. Therefore, it is less meaningful to find a solution for a particular realization of randomness. On the contrary, the statistics, such as mean and variance, of the solutions are more interesting. We refer to [4, 15, 16, 19, 27] for closely related imaging and wave propagation problems in random media, where the medium properties are modeled as random functions.

In the context of the inverse random source scattering problem, the goal is to deduce the statistical structure, such as the mean and the standard deviation or the variance of the source function, from physically realizable measurements of the radiated fields, such as the measurements taken on the boundaries. Although the deterministic counterpart has been extensively investigated from both mathematical and numerical viewpoints, little is known for the stochastic case, especially its computational aspect. A uniqueness result can be found in Devaney [11], where it is shown that the auto-correlation function of the random source is uniquely determined everywhere outside the source region by the auto-correlation function of the radiated field. Recently, a novel and efficient Wiener chaos expansion-based technique has been developed for modeling and simulation of spatially incoherent sources in photonic crystals by Badieirostami *et al* [3]. See Bao *et al* [5] for a related inverse medium scattering problem with a stochastic source. One may consult Kaipio and Somersalo [20] for statistical inversion theory for general random inverse problems.

This paper is an extension of the work [6], which considered the inverse random source scattering problem for the one-dimensional Helmholtz equation in a homogeneous background medium. For the homogeneous medium case, the solution for the direct problem is able to be analytically constructed by using the integrated solution method. Explicit inversion formulas can also be derived to connect the mean and the variance of the random source function to the Fourier transform of the measurements, which are implemented by the fast Fourier transform. Since explicit solutions will not be available any more for the inhomogeneous medium

case, the extension will be nontrivial and so the difference will be obvious from the work in [6].

The random source function, representing the electric current density, is assumed to have a compact support contained in a finite interval. The problem is modeled with an outgoing wave condition imposed on the lateral end points of the finite interval, which reduces the model to a second-order stochastic two-point boundary value problem. This model problem is converted into an equivalent first-order stochastic two-point boundary value problem, and is shown to have a unique pathwise solution. By using the fundamental matrix, an integral equation is constructed for the solution of the direct problem. By studying the expectation and variance of the integral equation, inversion formulas are deduced to reconstruct the mean and variance of the random source function. Numerical examples are included to demonstrate the validity and effectiveness of the proposed method.

The paper is organized as follows. In section 2, we present the model problem and formulate it as a first-order two-point stochastic boundary value problem. The existence and uniqueness of the direct problem are established, and the solution is derived based on the fundamental matrix. We derive four integral equations, which build the construction formulas for the mean and the variance of the source function. In section 3, we discuss numerical implementation of the method and present three numerical examples to demonstrate the validity and effectiveness of the proposed approach. We conclude this paper with general remarks and directions for future research in section 4.

2. Inverse random source problem

In this section, we introduce a mathematical model for the inverse random source scattering problem. The model problem is first converted into a stochastic two-point boundary value problem. A theoretical framework for the direct model problem is established and reconstruction formulas are deduced for the solution of the inverse problem.

2.1. The model problem

Let $u(x)$ be the time-harmonic wave field at location x with the time factor $\mathrm{e}^{-\mathrm{i}\omega t}$ omitted and assume that the slab occupies the interval $[0, 1]$. Then the wave field u satisfies the one-dimensional Helmholtz equation

$$u''(x, \omega) + \omega^2(1 + q(x))u(x, \omega) = f(x), \tag{2.1}$$

where the derivative is taken with respect to the spatial variable x, the magnetic permeability and the electric permittivity of the vacuum are assumed to be the unity for simplicity, $\omega > 0$ is the angular frequency, $q > 0$ implies the relative electric permittivity of the inhomogeneous medium and has a compact support in the interval $[0, 1]$, and f, representing the electric current density, is a stochastic source function, which is assumed to have the form

$$f(x) = g(x) + h(x)W_x'.$$

Here g and h are the deterministic functions with compact supports contained in the interval of the slab $[0, 1]$, W_x is a one-dimensional spatial Wiener process, and W_x' is its stochastic differential in the Itô sense which is commonly used as a model for the white noise, i.e. a spatial Gaussian random field. Throughout the paper, we assume that f, g, and h are the bounded functions in $[0, 1]$, i.e. $f, g, h \in L^\infty[0, 1]$. Following from the standard stochastic theory on the white noise, we have

$$\mathbb{E}[f(x)] = g(x) \qquad \text{and} \qquad \mathbb{V}[f(x)] = h^2(x),$$

where $\mathbb{E}$ and $\mathbb{V}$ are the expectation and variance operators, respectively. Thus g stands for the mean value of the random source function and h characterizes the size of the fluctuation for the random source. Obviously, due to the random nature of the source function, the solution u, the radiate field, is also a random function. Typical boundary conditions imposed on u are the so-called outgoing radiation boundary conditions, which are equivalent to the boundary conditions at two lateral end points of the interval $[0, 1]$:

$$u'(0, \omega) + \mathrm{i}\omega u(0, \omega) = 0 \qquad \text{and} \qquad u'(1, \omega) - \mathrm{i}\omega u(1, \omega) = 0. \tag{2.2}$$

Remark 2.1. The Wiener process is one of the two fundamental examples (the Poisson process is the simpler of the two) in the theory of continuous stochastic processes. Although we only consider Gaussian random field driven by the Wiener process in this paper, the strategy can be extended to other types of randomness in the source function with minor modifications. For the completeness of the paper, some preliminaries, including the Wiener process and stochastic Itô integral, are briefly presented in the appendix.

There are usually two types of problems posed for the above equations. Given the mean g and the standard deviation h of the random source function f, the direct problem is to determine the random wave field u. On the contrary, the inverse source problem is to determine the mean value g and the standard deviation h or the variance h^2 of the random source from the boundary measurements of the random wave field $u(0, \omega)$, which is available for a sequence of angular frequencies ω. Our goal is to investigate both the direct and inverse problems, and particularly propose a novel and efficient numerical algorithm to solve the inverse source problem. Although we use the radiated field measured at the left boundary point $x = 0$ in our discussion, all of the results are still true if the measurements are taken at the right boundary point $x = 1$.

First, we show that the direct problem has a unique pathwise solution for each realization of the random field $\mathrm{d}W_x$, and the solution serves as the foundation of our numerical algorithm for the inverse problem. To begin with, we convert the second-order wave equation in the direct problem into a first-order two-point stochastic boundary value problem.

Let $u_1 = u$ and $u_2 = u'$, the second-order stochastic boundary value problem (2.1)–(2.2) can be equivalently written as a first-order two-point boundary value problem:

$$\mathrm{d}\mathbf{u} = (M\mathbf{u} + \mathbf{g})\,\mathrm{d}x + \mathbf{h}\,\mathrm{d}W_x, \tag{2.3}$$

$$A_0\mathbf{u}(0) = 0, \tag{2.4}$$

$$B_1\mathbf{u}(1) = 0, \tag{2.5}$$

where

$$\mathbf{u} = \begin{bmatrix} u_1 \\ u_2 \end{bmatrix}, \qquad \mathbf{g} = \begin{bmatrix} 0 \\ g \end{bmatrix}, \qquad \mathbf{h} = \begin{bmatrix} 0 \\ h \end{bmatrix}, \qquad M = \begin{bmatrix} 0 & 1 \\ -\omega^2(1+q) & 0 \end{bmatrix},$$

and

$$A_0 = [\mathrm{i}\omega 1], \qquad B_1 = [-\mathrm{i}\omega 1].$$

We use this equivalent problem to establish our analysis and deduce reconstruction formulas in the rest of this section.

2.2. *Two-point boundary value problem*

To solve the two-point boundary value problem, we treat it as a standard initial value problem at the left boundary point, $x = 0$, and then enforce the solution to satisfy the boundary condition at the right boundary point, $x = 1$. The reader is referred to Nualart and Pardoux [24], Ocone and Pardoux [25] for discussions on general boundary value problems for stochastic differential equations.

Consider the general first-order linear stochastic differential equation

$$\mathrm{d}\mathbf{u} = (M\mathbf{u} + \mathbf{g})\,\mathrm{d}x + \mathbf{h}\,\mathrm{d}W_x, \tag{2.6}$$

together with the boundary conditions given in the form of linear equations:

$$A_0\mathbf{u}_0 = \mathbf{v}_0, \tag{2.7}$$

$$B_1\mathbf{u}_1 = \mathbf{v}_1, \tag{2.8}$$

where $\mathbf{u}(x) \in \mathbb{C}^n$, $\mathbf{g}(x) \in \mathbb{C}^n$, and $\mathbf{h}(x) \in \mathbb{C}^n$ are n-dimensional vector fields, $\mathbf{v}_0 \in \mathbb{C}^{n_1}$ is a given n_1-dimensional vector field, $M(x) \in \mathbb{C}^{n\times n}$ is a matrix, $A_0 \in \mathbb{C}^{n_1\times n}$ is matrix, and $B_1 \in \mathbb{C}^{n_2\times n}$ and $\mathbf{v}_1 \in \mathbb{C}^{n_2}$ with $n_1 + n_2 = n$. For the general first-order stochastic boundary value problem (2.6)–(2.8), we give a necessary and sufficient condition for the pathwise existence and uniqueness of solution for any fixed realization of the Wiener process W_x.

We note that a solution to (2.6), if any, takes the form

$$\mathbf{u}(x) = \Phi(x)\left[\mathbf{u}_0 + \int_0^x \Phi^{-1}(y)\mathbf{g}(y)\,\mathrm{d}y + \int_0^x \Phi^{-1}(y)\mathbf{h}(y)\,\mathrm{d}W_y\right], \tag{2.9}$$

where the last expression is given in the sense of the Itô integral and Φ is the fundamental matrix of the nonautonomous system for the ordinary differential equation:

$$\Phi'(x) = M(x)\Phi(x), \qquad \Phi(0) = I. \tag{2.10}$$

Here I is the $n \times n$ identity matrix.

Evaluating (2.9) at $x = 1$ yields

$$\mathbf{u}(1) = \Phi(1)\left[\mathbf{u}_0 + \int_0^1 \Phi^{-1}(x)\mathbf{g}(x)\,\mathrm{d}x + \int_0^1 \Phi^{-1}(x)\mathbf{h}(x)\,\mathrm{d}W_x\right].$$

The solution is required to satisfy the boundary condition (2.8):

$$B_1\Phi(1)\left[\mathbf{u}_0 + \int_0^1 \Phi^{-1}(x)\mathbf{g}(x)\,\mathrm{d}x + \int_0^1 \Phi^{-1}(x)\mathbf{h}(x)\,\mathrm{d}W_x\right] = \mathbf{v}_1.$$

We denote the random vector

$$B_1\Phi(1)\int_0^1 \Phi^{-1}(y)\mathbf{h}(y)\,\mathrm{d}W_y = \mathbf{w} \in \mathbb{C}^n.$$

The well-posedness of the two-point stochastic boundary value problem (2.6)–(2.8) can be equivalently formulated as follows: given $\mathbf{v}_0$ and $\mathbf{v}_1$, for any random process $\mathbf{w}$, there exists a unique solution $\mathbf{u}_0$ to the linear equations

$$A_0\mathbf{u}_0 = \mathbf{v}_0,$$

$$B_1\Phi(1)\mathbf{u}_0 = \mathbf{v}_1 - \mathbf{w} - B_1\Phi(1)\int_0^1 \Phi^{-1}(y)\mathbf{g}(y)\,\mathrm{d}y.$$

It follows from the linear algebra that the unique solvability of the above linear system can be obtained if the coefficient matrix is nonsingular. Therefore we obtain the necessary and sufficient condition for the well-posedness of the two-point stochastic boundary value problem.

Theorem 2.1. *The two-point stochastic boundary value problem (2.6)–(2.8) has a unique solution if and only if*

$$\det\begin{bmatrix} A_0 \\ B_1\Phi(1) \end{bmatrix} \neq 0. \tag{2.11}$$

2.3. Reconstruction formulas

Using the theory developed in the previous subsection, we may obtain the existence and uniqueness for the direct source problem. Furthermore, the constructed proof deduces the reconstruction formulas for the inverse source scattering problem.

Before presenting the well-posedness of the direct problem, we have to verify that the solution of the fundamental matrix is invertible for any $x \in [0, 1]$ in the context of the scattering problem (2.1) and (2.2). In fact, it is easy to check that

$$[\det\Phi(x)]' = \operatorname{trace} M(x) \cdot \det\Phi(x) = 0,$$

which gives

$$\det\Phi(x) = \det\Phi(0) = 1.$$

Thus the fundamental matrix Φ is invertible for any $x \in [0, 1]$.

Corollary 2.1. *The two-point boundary value problem (2.3)–(2.5) attains a unique solution.*

Proof. Denote the 2×2 matrix

$$\Phi(1) = \begin{bmatrix} \phi_1 & \phi_2 \\ \phi_3 & \phi_4 \end{bmatrix}.$$

We have from the unity of the determinant for the fundamental matrix that

$$\det\Phi(1) = \phi_1\phi_4 - \phi_2\phi_3 = 1. \tag{2.12}$$

A simple calculation yields

$$\det\begin{bmatrix} A_0 \\ B_1\Phi(1) \end{bmatrix} = \begin{vmatrix} \mathrm{i}\omega & 1 \\ -\mathrm{i}\omega\phi_1 + \phi_3 & -\mathrm{i}\omega\phi_2 + \phi_4 \end{vmatrix} = (\omega^2\phi_2 - \phi_3) + \mathrm{i}\omega(\phi_1 + \phi_4).$$

Taking the square of the amplitude for the above determinant and substituting (2.12) yield

$$|(\omega^2\phi_2 - \phi_3) + \mathrm{i}\omega(\phi_1 + \phi_4)|^2 = \omega^4\phi_2^2 + \omega^2\left(\phi_1^2 + \phi_4^2 + 2\right) + \phi_3^2 > 0 \qquad \text{for all} \quad \omega > 0,$$

which implies that

$$\det\begin{bmatrix} A_0 \\ B_1\Phi(1) \end{bmatrix} \neq 0.$$

It follows from theorem 2.1 that the two-point boundary value problem (2.3)–(2.5) has a unique solution. □

Next we deduce the integral equations to reconstruct the mean and the variance of the random source function.

Recalling

$$\mathbf{u}(1) = \Phi(1)\left[\mathbf{u}_0 + \int_0^1 \Phi^{-1}(x)\mathbf{g}(x)\,\mathrm{d}x + \int_0^1 \Phi^{-1}(x)\mathbf{h}(x)\,\mathrm{d}W_x\right], \tag{2.13}$$

where $\mathbf{u}_0 = [u(0, \omega), -\mathrm{i}\omega u(0, \omega)]$ and $\mathbf{u}_1 = [u(1, \omega), \mathrm{i}\omega u(1, \omega)]$ due to the radiation condition (2.2).

To simply the derivation, we introduce the following notation:

$$\Phi(1) = \begin{bmatrix} \phi_1(\omega) & \phi_2(\omega) \\ \phi_3(\omega) & \phi_4(\omega) \end{bmatrix}, \qquad \Phi(1)\mathbf{u}_0 = \begin{bmatrix} v_1(\omega) \\ v_2(\omega) \end{bmatrix},$$

and

$$\Phi(1)\Phi^{-1}(x) = \begin{bmatrix} \psi_1(x,\omega) & \psi_2(x,\omega) \\ \psi_3(x,\omega) & \psi_4(x,\omega) \end{bmatrix},$$

where

$$v_1(\omega) = [\phi_1(\omega) - \mathrm{i}\omega\phi_2(\omega)]u(0,\omega),$$
$$v_2(\omega) = [\phi_3(\omega) - \mathrm{i}\omega\phi_4(\omega)]u(0,\omega).$$

Using the above notation, we may obtain the expressions of the two components in (2.13):

$$u_1(1,\omega) = v_1(\omega) + \int_0^1 \psi_2(x,\omega)g(x)\,\mathrm{d}x + \int_0^1 \psi_2(x,\omega)h(x)\,\mathrm{d}W_x \tag{2.14}$$

$$u_2(1,\omega) = v_2(\omega) + \int_0^1 \psi_4(x,\omega)g(x)\,\mathrm{d}x + \int_0^1 \psi_4(x,\omega)h(x)\,\mathrm{d}W_x. \tag{2.15}$$

It follows from the radiation condition (2.2) that

$$u_2(1,\omega) = \mathrm{i}\omega u_1(1,\omega),$$

which leads to the identity after substituting (2.14) and (2.15) into the above equation:

$$\int_0^1 [\psi_4(x,\omega) - \mathrm{i}\omega\psi_2(x,\omega)]g(x)\,\mathrm{d}x + \int_0^1 [\psi_4(x,\omega) - \mathrm{i}\omega\psi_2(x,\omega)]h(x)\,\mathrm{d}W_x$$
$$= \mathrm{i}\omega v_1(\omega) - v_2(\omega). \tag{2.16}$$

It will be helpful to split all the complex functions into the sum of real and imaginary parts in order to derive the variance reconstruction formulas. So denote

$$u(0,\omega) = \mathrm{Re}\,u(0,\omega) + \mathrm{iIm}\,u(0,\omega).$$

Separating the real and imaginary parts of (2.16) gives

$$\int_0^1 \psi_4(x,\omega)g(x)\,\mathrm{d}x + \int_0^1 \psi_4(x,\omega)h(x)\,\mathrm{d}W_x = \varphi_1(\omega), \tag{2.17}$$

$$\int_0^1 \psi_2(x,\omega)g(x)\,\mathrm{d}x + \int_0^1 \psi_2(x,\omega)h(x)\,\mathrm{d}W_x = \varphi_2(\omega), \tag{2.18}$$

where φ_1 and φ_2 are given in terms of the real and the imaginary parts of the measured field $u(0,\omega)$:

$$\varphi_1(\omega) = \mathrm{Re}[\mathrm{i}\omega v_1(\omega) - v_2(\omega)] = \mathrm{Re}[\omega^2\phi_2(\omega) - \phi_3(\omega) + \mathrm{i}\omega(\phi_1(\omega) + \phi_4(\omega))]u(0,\omega),$$
$$= [\omega^2\phi_2(\omega) - \phi_3(\omega)]\mathrm{Re}\,u(0,\omega) - \omega[\phi_1(\omega) + \phi_4(\omega)]\mathrm{Im}\,u(0,\omega),$$
$$\varphi_2(\omega) = -\frac{1}{\omega}\mathrm{Im}[\mathrm{i}\omega v_1(\omega) - v_2(\omega)] = -\frac{1}{\omega}\mathrm{Im}[\omega^2\phi_2(\omega) - \phi_3(\omega) + \mathrm{i}\omega(\phi_1(\omega) + \phi_4(\omega))]u(0,\omega)$$
$$= -\frac{1}{\omega}[\omega^2\phi_2(\omega) - \phi_3(\omega)]\mathrm{Im}\,u(0,\omega) - [\phi_1(\omega) + \phi_4(\omega)]\mathrm{Re}\,u(0,\omega).$$

Now $\varphi_1(\omega)$ and $\varphi_2(\omega)$ can be viewed as the measurement data corresponding to a sequence of angular frequency ω.

Taking the expectation on both sides of (2.17) and (2.18) and using the property of the Itô integral

$$\mathbb{E}\left[\int_0^1 \psi_2(x,\omega)h(x)\,\mathrm{d}W_x\right] = \mathbb{E}\left[\int_0^1 \psi_4(x,\omega)h(x)\,\mathrm{d}W_x\right] = 0,$$

we obtain the integral equations to reconstruct the mean of the random source function:

$$\int_0^1 \psi_4(x,\omega)g(x)\,\mathrm{d}x = \mathbb{E}[\varphi_1(\omega)], \tag{2.19}$$

$$\int_0^1 \psi_2(x,\omega)g(x)\,\mathrm{d}x = \mathbb{E}[\varphi_2(\omega)]. \tag{2.20}$$

Recalling the Itô isometry, we have

$$\mathbb{E}\left[\left(\int_0^1 \psi_4(x,\omega)h(x)\,\mathrm{d}W_x\right)^2\right] = \int_0^1 \psi_4^2(x,\omega)h^2(x)\,\mathrm{d}x,$$
$$\mathbb{E}\left[\left(\int_0^1 \psi_2(x,\omega)h(x)\,\mathrm{d}W_x\right)^2\right] = \int_0^1 \psi_2^2(x,\omega)h^2(x)\,\mathrm{d}x.$$

Taking the variance on both sides of (2.17) and (2.18), and using the above Itô isometry, we deduce the integral equations to reconstruct the variance of the random source function:

$$\int_0^1 \psi_4^2(x,\omega)h^2(x)\,\mathrm{d}x = \mathbb{V}[\varphi_1(\omega)], \tag{2.21}$$

$$\int_0^1 \psi_2^2(x,\omega)h^2(x)\,\mathrm{d}x = \mathbb{V}[\varphi_2(\omega)]. \tag{2.22}$$

Remark 2.2. In principle, both integral equations (2.19) and (2.20) can be used to reconstruct the mean of the random source function; both integral equation (2.21) and (2.22) can be used to reconstruct the variance of the random source function. In practice, the selection of one integral equation over another is determined by the singular values of the matrix obtained from the discretization of the integral kernel.

Remark 2.3. It is not hard to see that the data essentially require the knowledge of the quantity $\mathbb{E}[u(0,\omega)]$. According to the strong law of large numbers

$$\mathbb{P}\left[\lim_{m\to\infty} \frac{u_1(0,\omega)+\cdots+u_m(0,\omega)}{m} = \mathbb{E}[u(0,\omega)]\right] = 1,$$

where $u_i(0,\omega), i = 1,2,\ldots,m$ is for the ith measurement or realization, m is the total number of measurements or realizations, and $\mathbb{P}$ stands for the probability. The exact value of $\mathbb{E}[u(0,\omega)]$ will be obtained only if the measurement is taken at infinitely many times. Due to the finite number of realizations, the actual data will not be accurate and always have certain level of error.

Remark 2.4. In [6], an explicit formula is derived for the solution of the stochastic Helmholtz equation in the homogeneous medium based on the integrated solution method, which cannot be applied in the case of inhomogeneous media. However, the method introduced in this paper can easily handle the homogeneous medium and deduce the same solution as that from the method of the integrated solution.

In fact, in the homogeneous medium case, i.e. $q = 0$, the coefficient matrix M in the nonautonomous system (2.10) becomes a constant matrix. Thus, the fundamental matrix can be explicitly computed. Simple calculations yield

$$\Phi(1) = \begin{bmatrix} \cos\omega & \frac{1}{\omega}\sin\omega \\ -\omega\sin\omega & \cos\omega \end{bmatrix}, \qquad \Phi(1)\mathbf{u}_0 = u(0,\omega)\mathrm{e}^{-\mathrm{i}\omega}\begin{bmatrix} 1 \\ -\mathrm{i}\omega \end{bmatrix},$$

and

$$\Phi(1)\Phi^{-1}(x) = \begin{bmatrix} \cos[(1-x)\omega] & \frac{1}{\omega}\sin[(1-x)\omega] \\ -\omega\sin[(1-x)\omega] & \cos[(1-x)\omega] \end{bmatrix}.$$

Substituting above expressions into (2.14) and (2.15) we get

$$u_1(1,\omega) = u(0,\omega)\,\mathrm{e}^{-\mathrm{i}\omega} + \frac{1}{\omega}\int_0^1 \sin[(1-x)\omega]g(x)\,\mathrm{d}x + \frac{1}{\omega}\int_0^1 \sin[(1-x)\omega]h(x)\,\mathrm{d}W_x,$$

$$u_2(1,\omega) = -\mathrm{i}\omega u(0,\omega)\,\mathrm{e}^{-\mathrm{i}\omega} + \int_0^1 \cos[(1-x)\omega]g(x)\,\mathrm{d}x + \int_0^1 \cos[(1-x)\omega]h(x)\,\mathrm{d}W_x.$$

Recalling the radiation condition $u_2(1,\omega) = \mathrm{i}\omega u_1(1,\omega)$, we obtain the integral representation for the radiated field at $x = 0$ after combing the above two equations:

$$u(0,\omega) = \frac{1}{2\mathrm{i}\omega}\int_0^1 \mathrm{e}^{\mathrm{i}\omega x}g(x)\,\mathrm{d}x + \frac{1}{2\mathrm{i}\omega}\int_0^1 \mathrm{e}^{\mathrm{i}\omega x}h(x)\,\mathrm{d}W_x. \tag{2.23}$$

Once $u(0,\omega)$ is available, we may plug it into (2.9) and derive the explicit expression of the solution for the direct random source problem:

$$u(x,\omega) = \frac{1}{2\mathrm{i}\omega}\int_0^1 \mathrm{e}^{\mathrm{i}\omega|x-y|}g(y)\,\mathrm{d}y + \frac{1}{2\mathrm{i}\omega}\int_0^1 \mathrm{e}^{\mathrm{i}\omega|x-y|}h(y)\,\mathrm{d}W_y.$$

We refer to [6] for the detailed derivation of the inversion formulas to reconstruction the mean and variance of the random source function from (2.23).

3. Numerical experiments

In this section, we discuss the algorithmic implementation for the direct and inverse random source scattering problems, and present three numerical examples to demonstrate the validity and effectiveness of the proposed method.

3.1. Direct problem

First we comment on the scattering data and the direct solver for the one-dimensional stochastic Helmholtz equation. We refer to Cao *et al* [9] for the finite element and discontinuous Galerkin method for solving the two-dimensional stochastic Helmholtz equation, Higham [18] and Kloeden and Platen [21] for an account of various numerical methods and approximation schemes for general stochastic partial differential equations.

To generate the scattering data $u(0,\omega)$, it is required to solve the initial value problem (2.10) to numerically obtain the fundamental matrix, and the following linear system:

$$\begin{aligned} A_0\mathbf{u}_0 &= 0, \\ B_1\Phi(1)\mathbf{u}_0 &= -z - w, \end{aligned} \tag{3.1}$$

where w is a random number given in terms of the Itô integral

$$w = B_1\Phi(1)\int_0^1 \Phi^{-1}(x)h(x)\,\mathrm{d}W_x, \tag{3.2}$$

and z is a deterministic number given by the regular integral:

$$z = B_1\Phi(1)\int_0^1 \Phi^{-1}(x)\mathbf{g}(x)\,\mathrm{d}x. \tag{3.3}$$

Upon computing w and z, the scattering data can be analytically obtained from the solution of (3.1) by using the Gram rule:

$$u(0,\omega) = (z+w)/[(\omega^2\phi_2 - \phi_3) + \mathrm{i}\omega(\phi_1+\phi_4)]. \tag{3.4}$$

Note that the determinant is nonzero due to corollary 2.1.

The interval $[0, 1]$ was divided into n equal subintervals with nodes $x_j = jh$, $j = 0, 1, \ldots, n$, $h = 1/n$. The initial value problem (2.10) for the fundamental matrix is solved by the classic fourth-order Runge–Kutta formula:

$$\begin{aligned}
K_1 &= hM(x_j)\Phi_j,\\
K_2 &= hM\left(x_j+\tfrac{1}{2}h\right)\left(\Phi_j+\tfrac{1}{2}K_1\right),\\
K_3 &= hM\left(x_j+\tfrac{1}{2}h\right)\left(\Phi_j+\tfrac{1}{2}K_2\right),\\
K_4 &= hM(x_j+h)(\Phi_j+K_3),\\
\Phi_{j+1} &= \Phi_j + \tfrac{1}{6}(K_1+2K_2+2K_3+K_4),
\end{aligned}$$

where

$$M(x_j) = \begin{bmatrix} 0 & 1\\ -\omega^2(1+q(x_j)) & 0\end{bmatrix} \qquad \text{and} \qquad \Phi_0 = \begin{bmatrix}1 & 0\\ 0 & 1\end{bmatrix}.$$

The random number w is computed by using the definition of the Itô integral:

$$\begin{aligned}
w &= B_1\Phi(1)\int_0^1 \Phi^{-1}(x)h(x)\,\mathrm{d}W_x = \int_0^1 [\psi_4(x,\omega) - \mathrm{i}\omega\psi_2(x,\omega)]h(x)\,\mathrm{d}W_x\\
&\approx \sum_{j=1}^{n-1}[\psi_4(x_j,\omega) - \mathrm{i}\omega\psi_2(x_j,\omega)]h(x_j)\,\mathrm{d}W_j,
\end{aligned}$$

where the spatial Brownian motion $\mathrm{d}W_j = \xi_j/\sqrt{n}$, in which $\xi_j \in N(0, 1)$ is a random variable in the standard Gaussian distribution with zero mean and unit variance. We generate ξ_j by a random number generator in FORTRAN90. The deterministic number z is computed by a regular numerical quadrature:

$$\begin{aligned}
z &= B_1\Phi(1)\int_0^1 \Phi^{-1}(x)\mathbf{g}(x)\,\mathrm{d}x = \int_0^1 [\psi_4(x,\omega) - \mathrm{i}\omega\psi_2(x,\omega)]g(x)\,\mathrm{d}x\\
&\approx h\sum_{j=1}^{n-1}[\psi_4(x_j,\omega) - \mathrm{i}\omega\psi_2(x_j,\omega)]g(x_j).
\end{aligned}$$

Therefore, at each frequency ω, we solve the initial value problem (2.10) to obtain the fundamental matrix and compute the deterministic number z. The scattering data are then available from (3.4) after computing the random number w corresponding to some specific realization of the random variable.

3.2. Inverse problem

The inverse problem consists of recovering the mean g and variance h^2 from the data function in terms of the $u(0, \omega)$. In section 2.3, two integral equations are derived for the reconstruction of the mean and the variance, respectively. Both of the integral equations are implemented by

using the pseudo-inverse solution in order to compare the results, and provide us a criterion to choose one integral equation over another one.

Let T denote the linear operator with kernel $T(x, \omega)$ standing for $\psi_2(x, \omega)$ in (2.19) or $\psi_4(x, \omega)$ in (2.20), or for $\psi_2^4(x, \omega)$ in (2.21) or $\psi_4^2(x, \omega)$ in (2.22). We briefly introduce the singular value decomposition (SVD) of the linear operator. The SVD of T is a representation of the form

$$T(x, \omega) = \sum_{j=1}^{\infty} \sigma_j u_j(x) v_j^*(\omega),$$

where σ_j is the singular value associated with the singular functions u_j and v_j. The pseudo-inverse solution to the integral equations (2.19)–(2.20) or (2.21)–(2.22) generates the minimal norm solution. The SVD of T may be used to express the generalized inverse T^+ as

$$T^+(x, \omega) = \sum_{j=1}^{\infty} \frac{1}{\sigma_j} v_j(\omega) u_j^*(x).$$

In order to avoid the numerical instability, the SVD inversion formulas must be regularized. In particular, $1/\sigma$ is replaced in the above generalized inverse by $R(\sigma)$, where $R(\sigma)$ is a suitable regularizer. The role of regularization is to limit the contribution of small singular values to the reconstruction. This has the effect of replacing an ill-posed problem with a well-posed one that closely approximates the original one. A simple choice for $R(\sigma)$ consists of truncation, i.e.

$$R(\sigma) = \begin{cases} \sigma^{-1} & \text{for } \sigma \geqslant \varepsilon \\ 0 & \text{for } \sigma < \varepsilon \end{cases},$$

where $\varepsilon > 0$ is a regularized parameter. Let the sequence of the truncated singular values be arranged in a decreasing order:

$$\sigma_{\max} \geqslant \cdots \geqslant \sigma_{\min} \geqslant \varepsilon > 0,$$

i.e. $\sigma_{\max}$ is the largest singular value and $\sigma_{\min}$ is the smallest singular value which is greater than the given regularization parameter. Define a reference number $\rho = \sigma_{\max}/\sigma_{\min}$, which is the ratio between the largest and smallest singular valued, and will provide us a criterion on how to choose the integral equations for the inversions. In the following three numerical examples, the scatterer function, representing the inhomogeneous medium, is taken as

$$q(x) = \exp\left[-\frac{\pi^2(2x-1)^2}{0.64}\right].$$

Example 1. Reconstruct the mean and the standard deviation given by

$$g_1(x) = \sin(2\pi x) \qquad \text{and} \qquad h_1(x) = 0.5 - 0.5\cos(2\pi x)$$

inside the interval $[0, 1]$. See figure 1 for the random source function $f(x) = g_1(x) + h_1(x)\, \mathrm{d}W_x$ corresponding to a realization of the randomness. This is a simple example as both functions g_1 and h_1 contain very few low frequency Fourier modes. For the reconstruction of the mean value g_1 and the variance h_1^2, the scattering data $u(0, \omega_j)$ are computed at discrete frequencies $\omega_j = \omega_{\min} + j(\omega_{\max} - \omega_{\min})/k$, $j = 0, 1, \ldots, k$, where $\omega_{\min} = 1.0$, $\omega_{\max} = 7.0$, and $k = 6$.

Table 1 shows some parameters, such as the regularization parameter ε for the truncated SVD, largest and smallest singular values $\sigma_{\max}$ and $\sigma_{\min}$, and the reference number ρ as the ratio between the largest singular value and the smallest singular value, related to the SVD of the

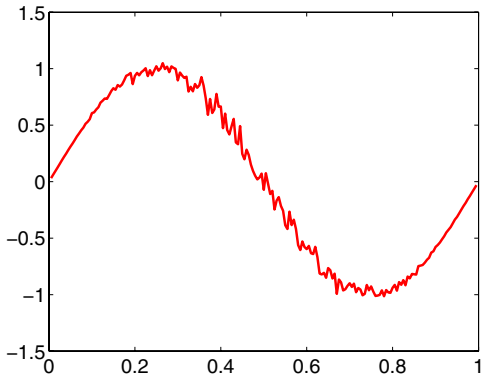

Figure 1. The random source function f for example 1.

Table 1. Example 1. Truncated SVD of the four integral kernels for the mean and variance.

	Mean		Variance	
	ψ_2	ψ_4	ψ_2^2	ψ_4^2
ε	0.10	0.10	0.10	0.10
$\sigma_{\max}$	6.18	11.56	3.50	12.83
$\sigma_{\min}$	0.90	1.24	0.17	0.64
ρ	6.86	9.32	20.59	20.04

integral kernels corresponding to the functions $\psi_2(x, \omega)$, $\psi_4(x, \omega)$, $\psi_2^2(x, \omega)$, and $\psi_4^2(x, \omega)$, respectively. The regularization parameter ε is chosen mainly based on an observation of the distribution for the singular values. Usually it is taken as a positive number between two consecutive singular values with a big gap.

Figure 2 plots the singular values of the matrices corresponding to the integral kernels $\psi_2(x, \omega)$ and $\psi_4(x, \omega)$ in (2.19) and (2.20), which are the reconstruction formulas for the mean. Figure 3 shows the reconstructed mean against the exact ones with the number of realization $m = 10^4$. The relative error of the reconstruction is $e = 4.13 \times 10^{-2}$ by using the integral equation (2.19), while the relative error of the reconstruction $e = 2.30 \times 10^{-1}$ by using the integral equation (2.20). Obviously the inversion result from the integral kernel ψ_2 is better than that from the integral kernel ψ_4. In fact, it can be confirmed by observing the reference numbers: $\rho = 6.86$ for the integral kernel ψ_2, while $\rho = 9.32$ for the integral kernel ψ_4. The reference number plays the role of the condition number for a matrix, which reflects the ill-posedness of the problem. The smaller the reference number is, the more well-posed the problem will be. Hence, it will be more reliable for the inversion by choosing the equation with a smaller reference number.

Figure 4 plots the singular values of the matrices discretized from the integral kernels $\psi_2^2(x, \omega)$ and $\psi_4^2(x, \omega)$ in (2.21) and (2.22), which are the reconstruction formulas for the variance. Figure 5 shows the reconstructed variance against the exact ones with the number of realization $m = 10^4$. The relative errors are on the same level: $e = 3.65 \times 10^{-2}$ by using the kernel ψ_2^2 and $e = 3.72 \times 10^{-2}$ by using the kernel ψ_4^2, which is not surprising at all. If we compare the reference numbers for the variance in table 1: one is $\rho = 20.59$ and another

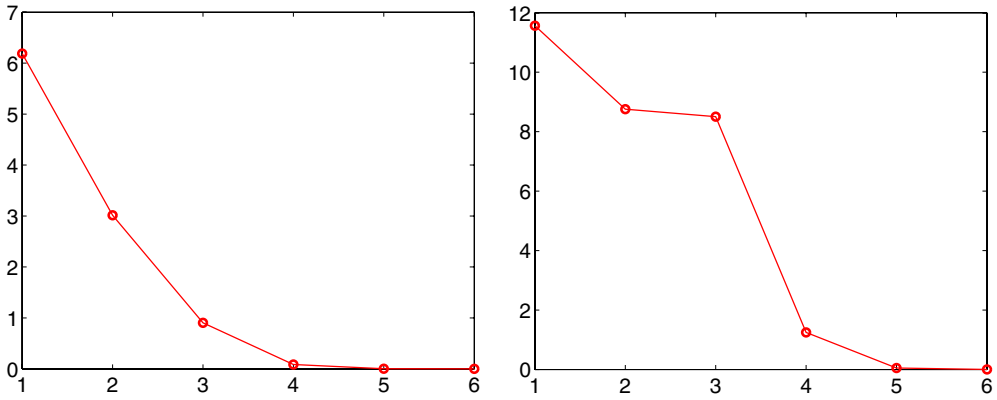

Figure 2. Singular values for example 1: (left) ψ_2; (right) ψ_4.

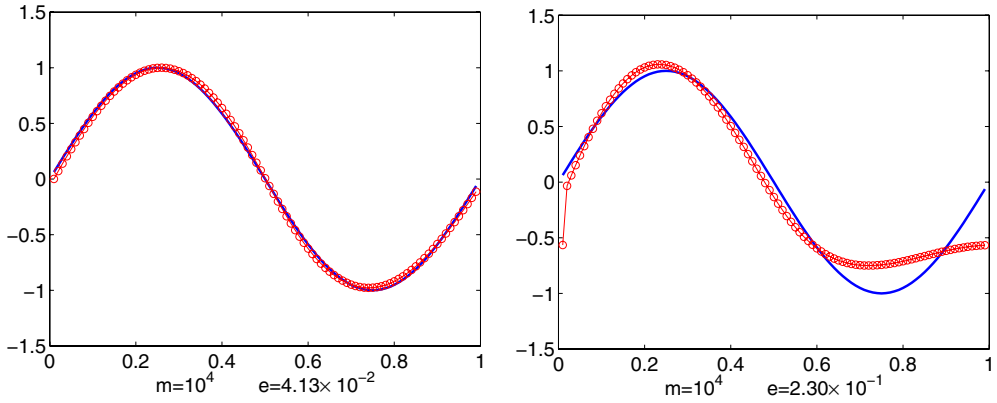

Figure 3. Reconstruction of the mean for example 1: (left) ψ_2; (right) ψ_4.

is $\rho = 20.04$. The reference numbers imply that the reconstructions should not have much differences by using either ψ_2^2 or ψ_4^2 since they are very close.

The reconstructed results are almost indistinguishable from the exact functions from the graphs even for the number of realizations $m = 10^4$ if the right equations are chosen for the inversions. It is obvious that the better reconstructions may be obtained when the more accurate data are used, i.e. larger number of realizations.

Example 2. Let

$$g(x) = 0.3\left[(1-\cos(2x)) - \tfrac{16}{21}(1-\cos(3x)) + \tfrac{5}{28}(1-\cos(4x))\right],$$
$$h(x) = 0.6 - 0.3\cos(x) - 0.3\cos(2x),$$

reconstruct the mean and the standard deviation given by

$$g_2(x) = g(2\pi x) \qquad \text{and} \qquad h_2(x) = h(2\pi x)$$

inside the interval $[0, 1]$. See figure 6 for the random source function $f(x) = g_2(x)+h_2(x)\,\mathrm{d}W_x$ corresponding to a realization of the randomness. This example is a little more complicated than example 1 since both functions contain more higher frequency modes. Correspondingly,

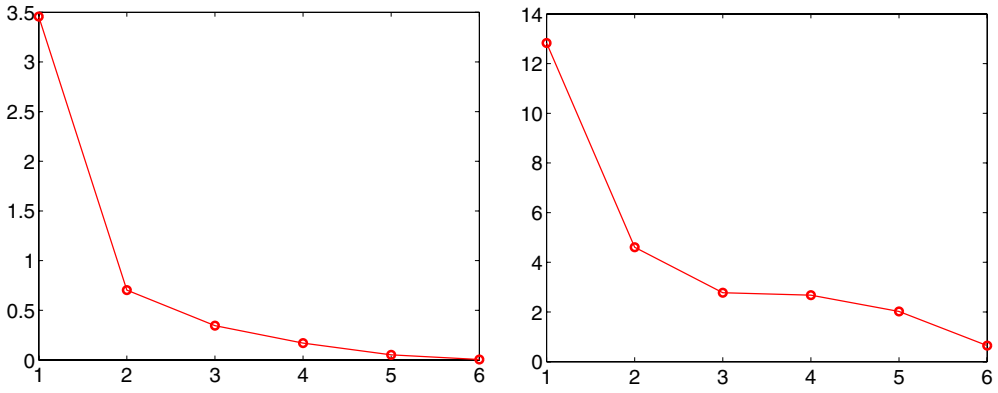

Figure 4. Singular values for example 1: (left) ψ_2^2; (right) ψ_4^2.

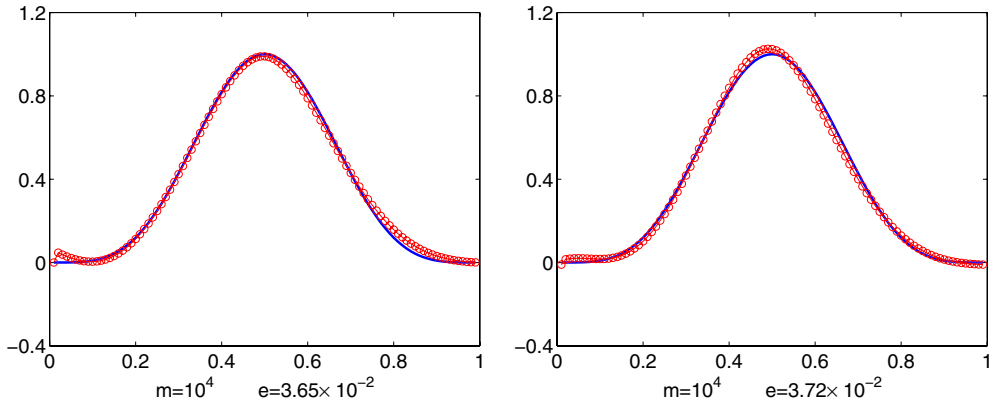

Figure 5. Reconstruction of the variance for example 1: (left) ψ_2^2; (right) ψ_4^2.

the data at high frequencies should be computed to recover the mean g_2 and the standard deviation h_2. For the reconstruction of the mean value g_2, the scattering data $u(0, \omega_j)$ are computed at discrete frequencies $\omega_j = \omega_{\min} + j(\omega_{\max} - \omega_{\min})/k$, $j = 0, 1, \ldots, k$, where $\omega_{\min} = 1.0$, $\omega_{\max} = 31.0$, and $k = 20$; while the scattering data $u(0, \omega_j)$ are computed at frequencies $\omega_j = \omega_{\min} + j(\omega_{\max} - \omega_{\min})/k$, $j = 1, 2, \ldots, k$, where $\omega_{\min} = 1.0$, $\omega_{\max} = 11.0$, and $k = 10$, for the reconstruction of the standard deviation h_2.

Table 2 shows the regularization parameter, largest and smallest singular values, and the reference numbers for the truncated SVD of the kernels corresponding to $\psi_2(x, \omega)$, $\psi_4(x, \omega)$, $\psi_2^2(x, \omega)$, and $\psi_4^2(x, \omega)$, respectively.

Figures 7 and 8 plot the singular values of the matrices corresponding to the integral kernels $\psi_2(x, \omega)$ and $\psi_4(x, \omega)$ in (2.19) and (2.20), and $\psi_2^2(x, \omega)$ and $\psi_4^2(x, \omega)$ in (2.21) and (2.22), respectively. Figures 9 and 10 show the reconstructed mean and variance against the exact ones with the number of realization $m = 10^4$. The relative reconstruction errors are $e = 6.06 \times 10^{-2}$ (using ψ_2 to reconstruct the mean) and $e = 5.08 \times 10^{-2}$ (using ψ_4 to reconstruct the mean), and $e = 1.47 \times 10^{-1}$ (using ψ_2^2 to reconstruct the variance) and $e = 6.78 \times 10^{-2}$ (using ψ_4^2 to reconstruct the variance). Again, it is confirmed from the

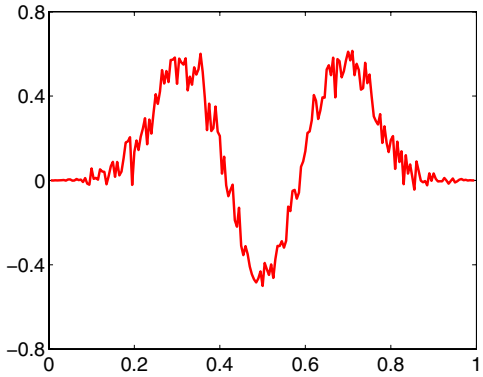

Figure 6. The random source function f for example 2.

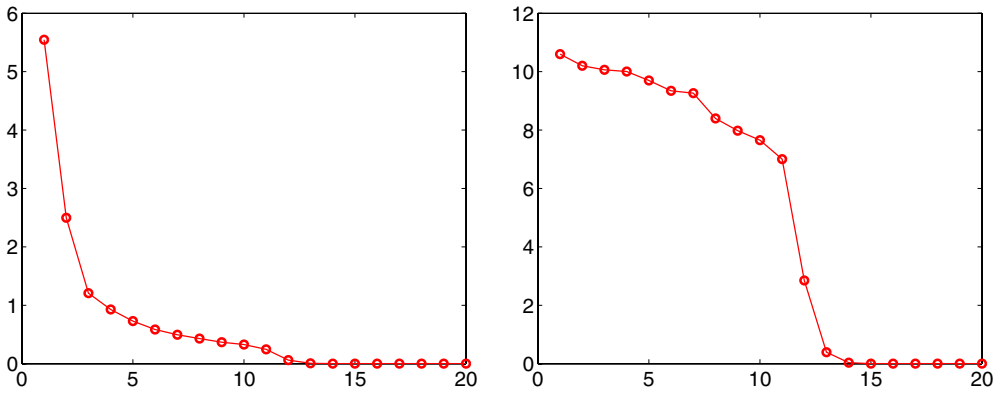

Figure 7. Singular values for example 2: (left) ψ_2; (right) ψ_4.

Table 2. Example 2. Truncated SVD of the four integral kernels for the mean and variance.

	Mean		Variance	
	ψ_2	ψ_4	ψ_2^2	ψ_4^2
ε	0.10	0.50	0.04	0.10
$\sigma_{\max}$	5.54	10.59	3.46	16.28
$\sigma_{\min}$	0.24	2.85	0.04	0.56
ρ	23.08	3.71	86.50	29.07

numerical results that better reconstructions can be obtained when using the equation with a smaller reference number than that with a larger reference number.

Example 3. Let

$$g(x) = 0.4\left[(1-\cos(3x)) - \tfrac{1215}{2783}(1-\cos(11x)) + \tfrac{7}{23}(1-\cos(12x))\right],$$
$$h(x) = 0.5e^{1} - 0.3e^{\cos(2x)} - 0.2e^{\cos(3x)},$$

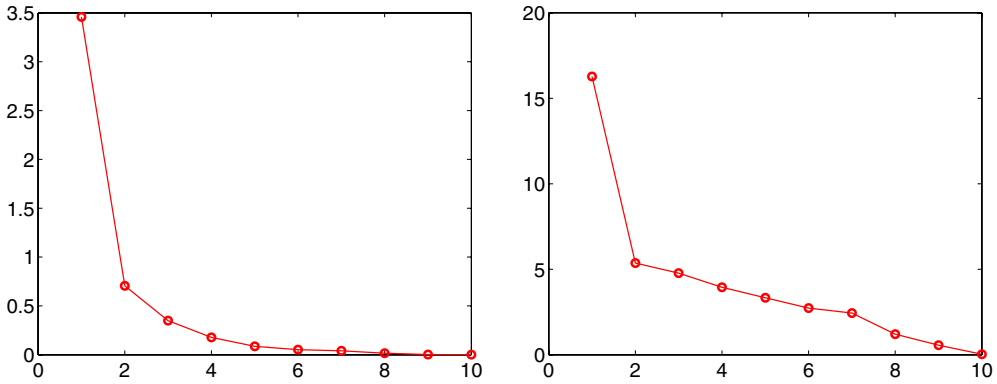

Figure 8. Singular values for example 2: (left) ψ_2^2; (right) ψ_4^2.

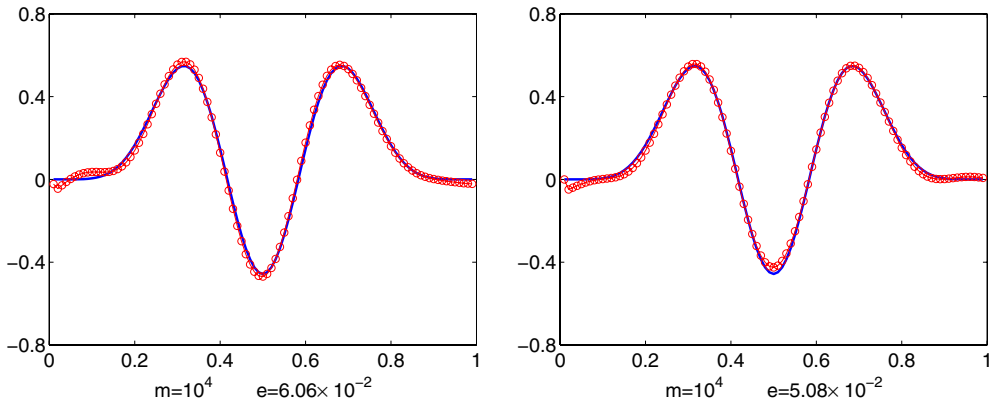

Figure 9. Reconstruction of the mean for example 2: (left) ψ_2; (right) ψ_4.

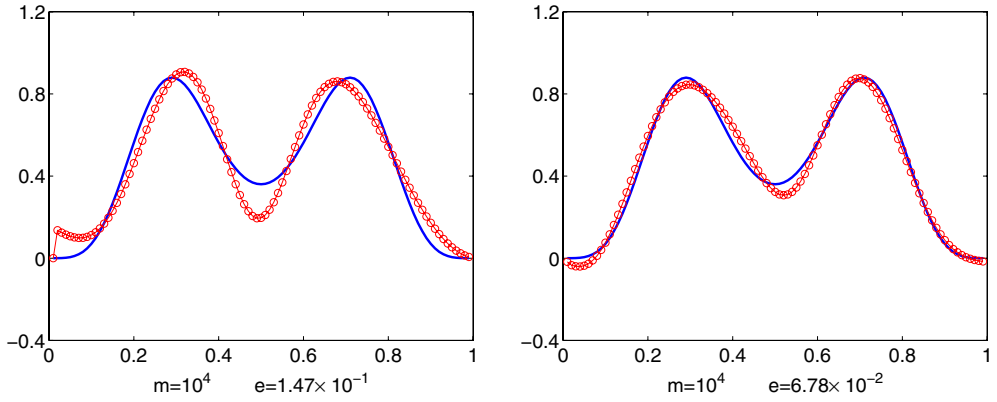

Figure 10. Reconstruction of the variance for example 2: (left) ψ_2^2; (right) ψ_4^2.

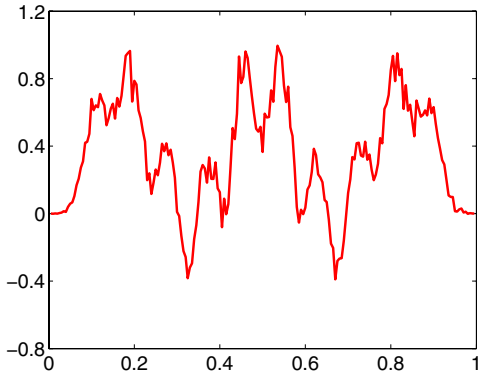

Figure 11. The random source function f for example 3.

Table 3. Example 3. Truncated SVD of the four integral kernels.

	Mean		Variance	
	ψ_2	ψ_4	ψ_2^2	ψ_4^2
ε	0.10	5.00	0.02	0.10
$\sigma_{\max}$	7.27	12.98	3.45	19.77
$\sigma_{\min}$	0.11	8.28	0.03	0.91
ρ	66.09	1.57	115.00	21.72

reconstruct the mean value and the standard deviation given by

$$g_3(x) = g(2\pi x) \qquad \text{and} \qquad h_3(x) = h(2\pi x)$$

inside the interval $[0, 1]$. See figure 11 for the random source function $f(x) = g_3(x) + h_3(x)\mathrm{d}W_x$ corresponding to a realization of the randomness. This example is clearly much more complicated than the previous two examples since both functions contain substantially more higher frequency modes. Therefore, the data at even higher frequencies should be computed to recover the mean g_3 and the standard deviation h_3. For the reconstruction of the mean value g_3, the scattering data $u(0, \omega_j)$ are computed at discrete frequencies $\omega_j = \omega_{\min} + j(\omega_{\max} - \omega_{\min})/k$, $j = 0, 1, \ldots, k$, where $\omega_{\min} = 1.0$, $\omega_{\max} = 91.0$, and $k = 40$; while the scattering data $u(0, \omega_j)$ are computed at frequencies $\omega_j = \omega_{\min} + j(\omega_{\max} - \omega_{\min})/k$, $j = 1, 2, \ldots, k$, where $\omega_{\min} = 1.0$, $\omega_{\max} = 17.0$, and $k = 17$, for the reconstruction of the standard deviation h_3.

Table 3 shows the regularization parameter, largest and smallest singular values, and the reference numbers for the truncated SVD of the kernels corresponding to $\psi_2(x, \omega)$, $\psi_4(x, \omega)$, $\psi_2^2(x, \omega)$, and $\psi_4^2(x, \omega)$, respectively. In this example, the differences in the reference numbers are obvious, which clearly suggests that the usage of the kernels ψ_4 and ψ_4^2 will generate better results than that of ψ_2 and ψ_2^2 for the inversion of the mean and variance, respectively.

Figures 12 and 13 plot the singular values of the matrices corresponding to the integral kernels $\psi_2(x, \omega)$ and $\psi_4(x, \omega)$ in (2.19) and (2.20), and $\psi_2^2(x, \omega)$ and $\psi_4^2(x, \omega)$ in (2.21) and (2.22), respectively. Figures 14 and 15 show the reconstructed mean and variance against the exact ones with the number of realization $m = 10^4$. The relative reconstruction errors

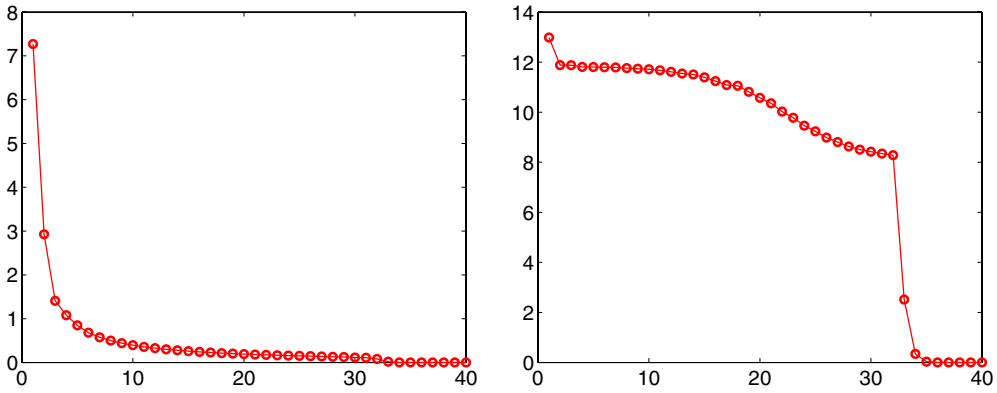

Figure 12. Singular values for example 3: (left) ψ_2; (right) ψ_4.

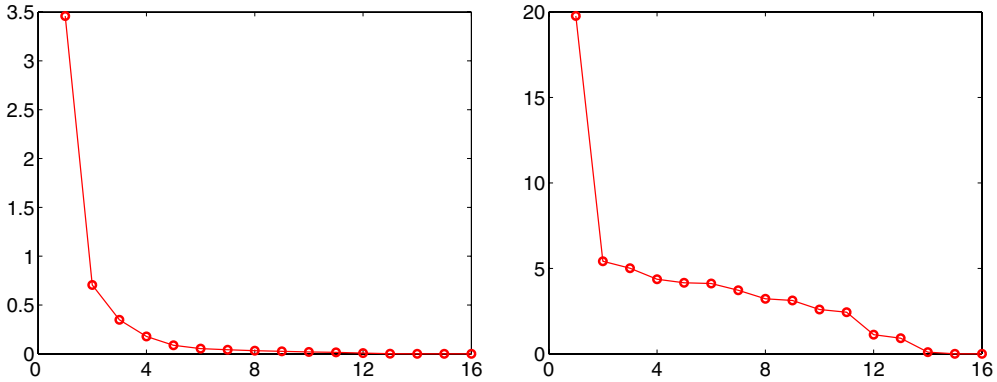

Figure 13. Singular values for example 3: (left) ψ_2^2; (right) ψ_4^2.

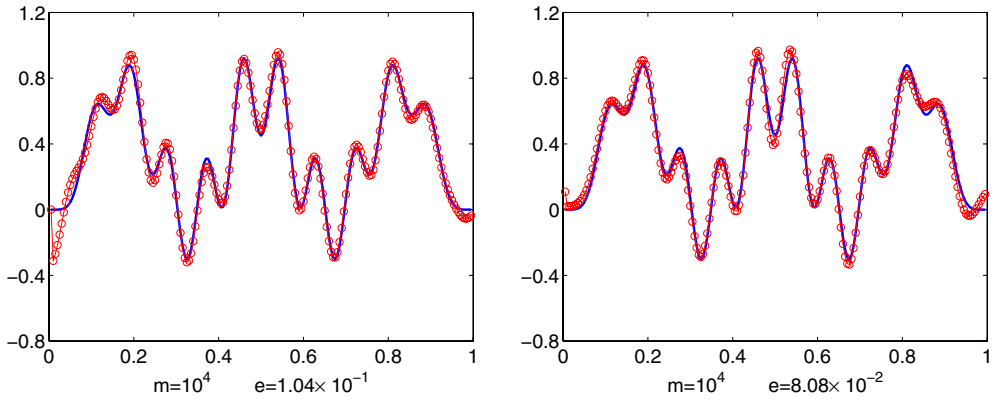

Figure 14. Reconstruction of the mean for example 3: (left) ψ_2; (right) ψ_4.

are $e = 1.01 \times 10^{-1}$ (using ψ_2 to reconstruct the mean) and $e = 8.08 \times 10^{-2}$ (using ψ_4 to reconstruct the mean), and $e = 1.07 \times 10^{-1}$ (using ψ_2^2 to reconstruct the variance) and $e = 7.77 \times 10^{-2}$ (using ψ_4^2 to reconstruct the variance). Once again, it is confirmed from the

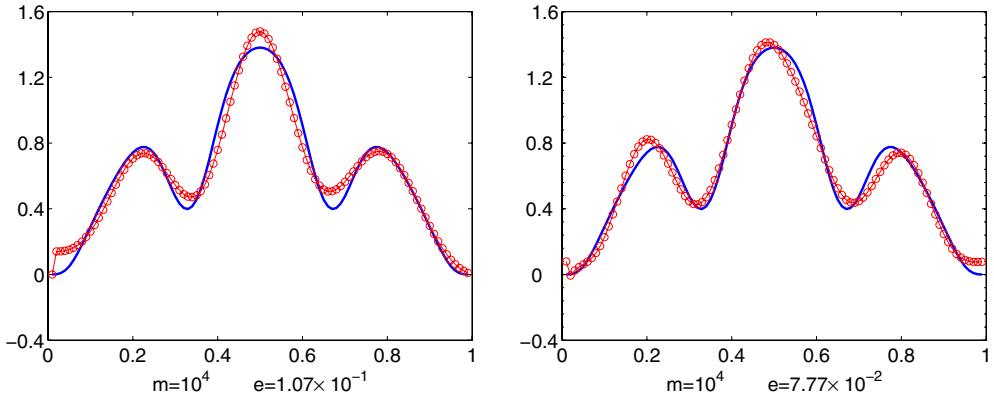

Figure 15. Reconstruction of the variance for example 3: (left) ψ_2^2; (right) ψ_4^2.

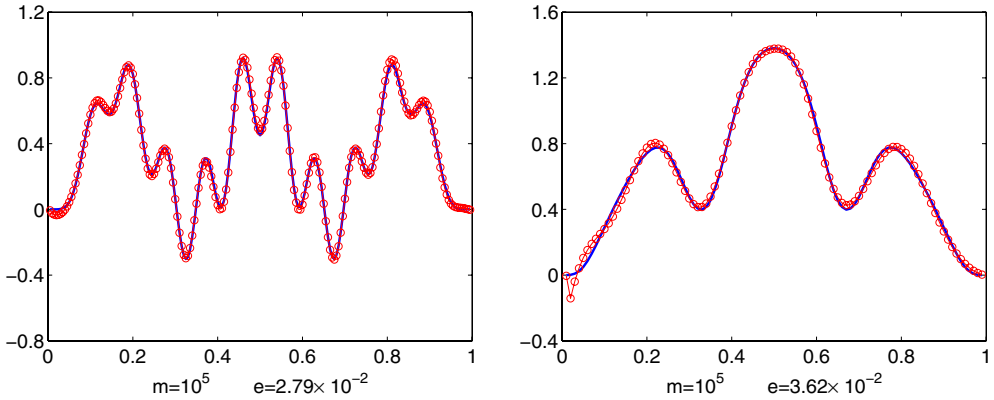

Figure 16. Reconstruction of the random source function for example 3 with the number of realization $m = 10^5$: (left) mean; (right) variance.

numerical results that better reconstructions can be obtained when using the equation with a smaller reference number than that with a larger reference number.

To show the effect of the number of the realization m on the reconstruction, figure 16 shows the reconstructed mean (using ψ_4) and variance (using ψ_4^2) against the exact ones with $m = 10^5$. The relative errors are $e = 2.79 \times 10^{-2}$ for the mean (comparing the error $e = 8.08 \times 10^{-2}$ when $m = 10^4$) and $e = 3.62 \times 10^{-2}$ for the variance (comparing the error $e = 7.77 \times 10^{-2}$ when $m = 10^4$). As expected, better results are obtained since a larger number of realization intends to reduce the effect of data error.

Finally, to test the stability of the method, we reconstruct the mean and variance with noisy data. Some relative random noise is added to the data, i.e. the scattering data take

$$u := (1 + \delta\,\mathrm{rand})u.$$

Here, rand gives uniformly distributed random numbers in $[-1, 1]$ and δ is a noise level parameter. Figure 17 displays the reconstructed mean and variance with the scattering data corresponding to the noisy level $\delta = 5\%$ and the number of the realization $m = 10^5$. It reconstructs the mean with a 8.81% relative error and the variance with a 5.86% relative error.

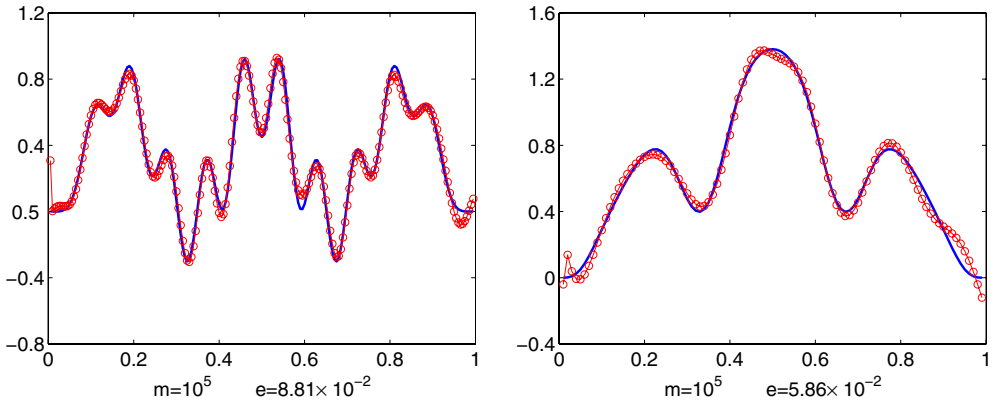

Figure 17. Reconstruction of the random source function for example 3 with noisy data: (left) mean; (right) variance.

An examination of the plot shows that the error of the reconstructions occurs largely around the edges, while the middle parts of the functions are recovered more accurately.

In summary, the following observations can be made based on numerical experiments. When the functions contain few low Fourier modes or fast decaying Fourier coefficients, accurate and stable reconstructions can be obtained easily by using scattering data with low frequencies. To get better results, scattering data containing high frequencies should be used to recover the functions with high Fourier modes. Generally, the system with a smaller reference number will generate a better construction and a more reliable solution due to a relatively well-posed nature of the problem.

4. Concluding remarks

We studied an inverse scattering problem for the stochastic Helmholtz equation with a random source function in a slab of the inhomogeneous medium. Both the direct and the inverse problems were considered. The direct problem was equivalently formulated as a two-point stochastic boundary value problem, and was shown having pathwise existence and uniqueness of a solution. Based on a constructed solution for the direct problem, the integral equations were derived for the reconstruction formulas, which connect the mean value and variance of the random source to those of the measured field. Numerical examples were presented to demonstrate the validity and effectiveness of the proposed method. We are currently investigating the inverse random source scattering problem for the two- and three-dimensional Helmholtz equation in homogeneous and inhomogeneous media and will report the progress elsewhere in the future.

Acknowledgments

The research was supported in part by NSF grants EAR-0724656, DMS-0914595, and DMS-1042958.

Appendix. Preliminaries

This section is a brief introduction to some notations for the stochastic differential equations. More details can be found in any good introductory book, for instance Øksendal [26] and Protter [28].

Let the triple $(\Omega, \mathcal{F}, P)$ be a complete probability space, where Ω is a given set called a sample space, $\mathcal{F}$ is a σ-algebra on Ω, and P is a probability measure on the measurable space $(\Omega, \mathcal{F})$. A random variable B is an $\mathcal{F}$-measurable function $B : \Omega \to \mathbb{R}$. Every random variable induces a probability measure μ_B on $\mathbb{R}$, defined by $\mu_B(U) = P[B^{-1}(U)]$ for $U \in \mathcal{F}$. Here μ_B is called the distribution of B. If $\int_\Omega |B(\xi)| \mathrm{d}P(\xi) < \infty$ then the number

$$\mathbb{E}[B] = \int_\Omega B(\xi)\, \mathrm{d}P(\xi) = \int_{\mathbb{R}} y\, \mathrm{d}\mu_B(y)$$

is called the expectation of B with respect to P.

A stochastic process is a parameterized collection of random variable $\{B_x\}_{x \in X}$ defined on the probability space $(\Omega, \mathcal{F}, P)$ and assuming values in $\mathbb{R}$. The parameter space X is usually the half-line $[0, \infty)$, but it may also be an interval $[a, b]$, as in this paper $[0, 1]$. Note that for each $x \in X$ fixed we have a random variable

$$\xi \to B_x(\xi); \qquad \xi \in \Omega.$$

On the other hand, fixing $\xi \in \Omega$ we can consider the function

$$x \to B_x(\xi); \qquad x \in X,$$

which is called a path of B_x.

The Brownian motion is an important example of the stochastic process, which is explained by the random collisions with the molecules of the liquid. In mathematics, Brownian motion is described by the Wiener process W_x, which is characterized by three facts: (1) $W_0 = 0$; (2) W_x is almost surely continuous; (3) W_x has independent increments with normal distribution of expected value zero and variance $x-y$, i.e. $W_x - W_y \sim N(0, x - y)$ for $0 \leqslant y \leqslant x$.

The Itô integral of a random function f is defined by

$$\int_a^b f(x, \xi)\, \mathrm{d}W_x(\xi) = \lim_{n \to \infty} \int_a^b f_n(x, \xi)\, \mathrm{d}W_x(\xi),$$

where W_x is the one-dimensional Wiener process, the limit is taken in $L^2(P)$, and $\{f_n\}$ is a sequence of elementary functions such that

$$\mathbb{E}\left[\int_a^b (f(x, \xi) - f_n(x, \xi))^2 \mathrm{d}x\right] \to 0 \qquad \text{as} \quad n \to \infty.$$

It can be shown that the Itô integral satisfies the mean zero:

$$\mathbb{E}\left[\int_a^b f(x, \xi)\, \mathrm{d}W_x\right] = 0$$

and the Itô isometry

$$\mathbb{E}\left[\left(\int_a^b f(x, \xi)\, \mathrm{d}W_x\right)^2\right] = \mathbb{E}\left[\int_a^b f^2(x, \xi)\, \mathrm{d}x\right].$$

References

[1] Albanese R and Monk P 2006 The inverse source problem for Maxwell's equations *Inverse Problems* **22** 1023–35
[2] Ammari H, Bao G and Fleming J 2002 An inverse source problem for Maxwell's equations in magnetoencephalography *SIAM J. Appl. Math.* **62** 1369–82
[3] Badieirostami M, Adibi A, Zhou H and Chow S 2007 Model for efficient simulation of spatially incoherent light using the Wiener chaos expansion method *Opt. Lett.* **32** 3188–90
[4] Bal G and Ryzhik L 2003 Time reversal and refocusing in random media *SIAM J. Appl. Math.* **63** 1475–98
[5] Bao G, Chow S-N, Li P and Zhou H 2010 Numerical solution of an inverse medium scattering problem with a stochastic source *Inverse Problems* **26** 074014
[6] Bao G, Chow S-N, Li P and Zhou H 2011 An inverse random source problem for the Helmholtz equation (in preparation)
[7] Bao G, Lin J and Triki F 2010 A multi-frequency inverse source problem *J. Diff. Eqns.* **249** 3443–65
[8] Bleistein N and Cohen J 1977 Nonuniqueness in the inverse source problem in acoustic and electromagnetics *J. Math. Phys.* **18** 194–201
[9] Cao Y-Z, Zhang R and Zhang K 2007 Finite element and discontinuous Galerkin method for stochastic Helmholtz equation in two- and three-dimensions *J. Comput. Math.* **26** 702–15
[10] Colton D and Kress R 1998 *Inverse Acoustic and Electromagnetic Scattering Theory (Appl. Math. Sci.* vol 93)2nd edn (Berlin: Springer)
[11] Devaney A 1979 The inverse problem for random sources *J. Math. Phys.* **20** 1687–91
[12] Devaney A, Marengo E and Li M 2007 The inverse source problem in nonhomogeneous background media *SIAM J. Appl. Math.* **67** 1353–78
[13] Devaney A and Sherman G 1982 Nonuniqueness in inverse source and scattering problems *IEEE Trans. Antennas Propag.* **30** 1034–7
[14] Eller M and Valdivia N 2009 Acoustic source identification using multiple frequency information *Inverse Problems* **25** 115005
[15] Fannjiang A C and Sølna K 2005 Superresolution and duality for time-reversal of waves in random media *Phys. Lett.* A **352** 22–9
[16] Fouque J-P, Garnier J, Papanicolaou G C and Sølna K 2007 *Wave Propagation and Time Reversal in Randomly Layered Media* (New York: Springer)
[17] Hauer K-H, Kühn L and Potthast R 2005 On uniqueness and non-uniqueness for current reconstruction from magnetic fields *Inverse Problems* **21** 955–67
[18] Higham D 2001 An algorithmic introduction to numerical simulation of stochastic differential equations *SIAM Rev.* **43** 525–46
[19] Ishimaru A 1978 *Wave Propagation and Scattering in Random Media* (New York: Academic)
[20] Kaipio J and Somersalo E 2005 *Statistical and Computational Inverse Problems* (New York: Springer)
[21] Kloeden P and Platen E 1992 *Numerical Solution of Stochastic Differential Equations* (New York: Springer)
[22] Marengo E and Devaney A 1999 The inverse source problem of electromagnetics: linear inversion formulation and minimum energy solution *IEEE Trans. Antennas Propag.* **47** 410–2
[23] Marengo E, Khodja M and Boucherif A 2008 Inverse source problem in nonhomogeneous background media: II. Vector formulation and antenna substrate performance characterization *SIAM J. Appl. Math.* **69** 81–110
[24] Nualart D and Pardoux E 1991 Boundary value problems for stochastic differential equations *Ann. Probab.* **19** 1118–44
[25] Ocone D and Pardoux E 1989 Linear stochastic differential equations with boundary conditions *Probab. Theory Relat. Fields* **82** 489–526
[26] Øksendal B 2005 *Stochastic Differential Equations: An Introduction with Applications* 6th edn (Berlin: Springer)
[27] Papanicolaou G 1971 Wave propagation in a one-dimensional random medium *SIAM J. Appl. Math.* **21** 13–8
[28] Protter P 2005 *Stochastic Integration and Differential Equations* 2nd edn (Berlin: Springer)
[29] Yuste R 2005 Fluorescence microscopy today *Nat. Methods* **2** 902–4